Effects of Horizontal Velocity Variations on Ultrasonic Velocity Measurements in Open Channels

By Eric D. Swain

Tallahassee, Florida
1992

U.S. DEPARTMENT OF THE INTERIOR
MANUEL LUJAN, JR., Secretary

U.S. GEOLOGICAL SURVEY
Dallas L. Peck, Director

CONTENTS

CONVERSION FACTORS, VERTICAL DATUM, AND ACRONYMS

Multiply	By	To obtain
inch (in.)	25.4	millimeter
inch per second (in/s)	25.4	millimeter per second
foot (ft)	0.3048	meter
foot per day (ft/d)	0.3048	meter per day
foot per second (ft/s)	0.3048	meter per second
mile (mi)	1.609	kilometer

Sea level: In this report "sea level" refers to the National Geodetic Vertical Datum of 1929—a geodetic datum derived from a general adjustment of the first-order level nets of the United States and Canada, formerly called Sea Level Datum of 1929.

Acronyms used in report:

UVM   ultrasonic velocity meter
AVM   acoustic velocity meter
1-D   one dimensional
2-D   two dimensional

DEFINITION OF SYMBOLS

Symbol	Definition
A	Cross-sectional area of canal
a	$u_*/\bar{u}\ k$
A_T	Cross-sectional area from channel center to acoustic transducer
A_H	Area of half channel
b	$\mathrm{Exp}\ (1\ +\ k\ \bar{u}/u_*)$
B	Length of acoustic path
c	1 in System International units and 1.49 in foot-pound units
β	Curve coefficient
d	Depth of water
d_c	Depth of water at channel center
ε	Coordinate line along which velocity is constant
ε_0	Coordinate line of zero velocity (channel bottom)
f	Darcy-Weisbach friction factor
f(x)	$\varepsilon_0 \left(1 - \dfrac{x}{T} \right)^{-\beta}$
K	Velocity correction factor defined by $\bar{u}/u_L$
k	von Karman's constant
n	Manning's friction coefficient
q(x)	Vertically averaged discharge per unit width at a distance x from centerline of channel
R	Hydraulic radius
t_{up}	Upstream traveltime
t_{dn}	Downstream traveltime
T	Distance from channel center to water edge
T_{DEOW}	Distance of transducer from edge of water
T_R	T_{DEOW}/T
T'	$T\left(1 - (\varepsilon_0)^{1/\beta} \right)$
Θ	Angle between streamflow and acoustic path
u	Water velocity
u(z)	Velocity at distance z from bottom at channel center
$\bar{u}$	Average velocity in cross section between channel center and transducer
$\bar{u}_H$	Average velocity in cross section between channel center and edge of water
u_*	Shear velocity
u_L	Acoustic line velocity
v	Point velocity
v_p	Velocity at a point on the acoustic path
w	Width of channel between transducers
x	Horizontal distance from channel center
y	Vertical distance from bottom of channel
y_0	Distance from channel bottom to point of zero velocity (boundary layer thickness)
z	Vertical distance from elevation of bottom at channel center
z_T	Vertical distance from channel bottom in the center to the level of the acoustic transducer path

Effects of Horizontal Velocity Variations on Ultrasonic Velocity Measurements in Open Channels

By Eric D. Swain

Abstract

Use of an ultrasonic velocity meter to determine discharge in open channels involves measuring the velocity in a line between transducers in the stream and relating that velocity to the average velocity in the stream. The standard method of calculating average velocity in the channel assumes that the velocity profile in the channel can be represented by the one-dimensional von Karman universal velocity profile. However, the velocity profile can be described by a two-dimensional equation that accounts for the horizontal velocity variations induced by the channel sides.

An equation to calculate average velocity accounts for the two-dimensional variations in velocity within a stream. The use of this new equation to calculate average velocity was compared to the standard method in theoretical trapezoidal cross sections and in the L-31N and Snapper Creek Extension Canals near Miami, Florida. These comparisons indicate that the two-dimensional variations have the most significant effect in narrow, deep channels. Also, the two-dimensional effects may be significant in some field situations and need to be considered when determining average velocity and discharge with an ultrasonic velocity meter.

INTRODUCTION

The discharge in an open channel can be determined by converting measurements of selected point velocities made by a mechanical current meter into an average velocity through a given channel cross section and multiplying this velocity by the area of that cross section. However, mechanical current meters are not considered accurate for velocities less than 0.2 ft/s (Rantz and others, 1982, p. 86). Accurate discharge measurements in the Levee-31N (L-31N) Canal and the Snapper Creek Extension Canal in south Florida (fig. 1) were required as part of a study to quantify canal leakage. Because velocities in these canals can be less than 0.1 ft/s, an ultrasonic velocity meter (UVM), sometimes referred to as an acoustic velocity meter (AVM), was considered an appropriate alternative to a mechanical current meter or an electromagnetic point-velocity meter.

Determination of average velocity in the channel cross section from measured velocity at a known depth requires knowledge of the velocity profile in the cross section or some assumption thereof. It is commonly assumed that the vertical velocity profile can be represented by the standard von Karman universal velocity profile (French, 1985) throughout the entire width of the channel. This von Karman velocity profile represents the effect of friction from the channel bottom on the velocity in the downstream direction at differing distances above the bottom. Only variations in velocities at differing vertical positions are represented; therefore, the standard von Karman velocity profile is termed the 1-D von Karman velocity profile. This velocity profile is accurate when the sole source of friction is the channel bottom, but near the banks, the friction from the channel sides also affects the velocity profile. If the channel is very wide, the side friction will not have a significant effect for most of the channel width, and the 1-D von Karman velocity profile will be a good approximation. However, the L-31N and Snapper Creek Extension Canals are probably not wide enough for side friction to be entirely neglected. The L-31N Canal has an average top width of about 100 ft and a maximum depth of 17 ft. The Snapper Creek Extension Canal is about 80 ft wide and has a sloping bottom with maximum depths of 16 to 35 ft.

When the channel is narrow and deep, vertical velocity profiles may be influenced, especially near the sides, by variations in the horizontal dimension due to channel-side friction. This differs from the assumption that the 1-D von Karman profile can be used as a basis to determine average cross-sectional velocity from the measured acoustic-line velocity. An equation that accounts for both vertical and horizontal effects (2-D) of friction on the downstream velocity can be derived. This equation can then be used to determine average cross-sectional velocity from measured acoustic-line velocity for a narrow, deep channel.
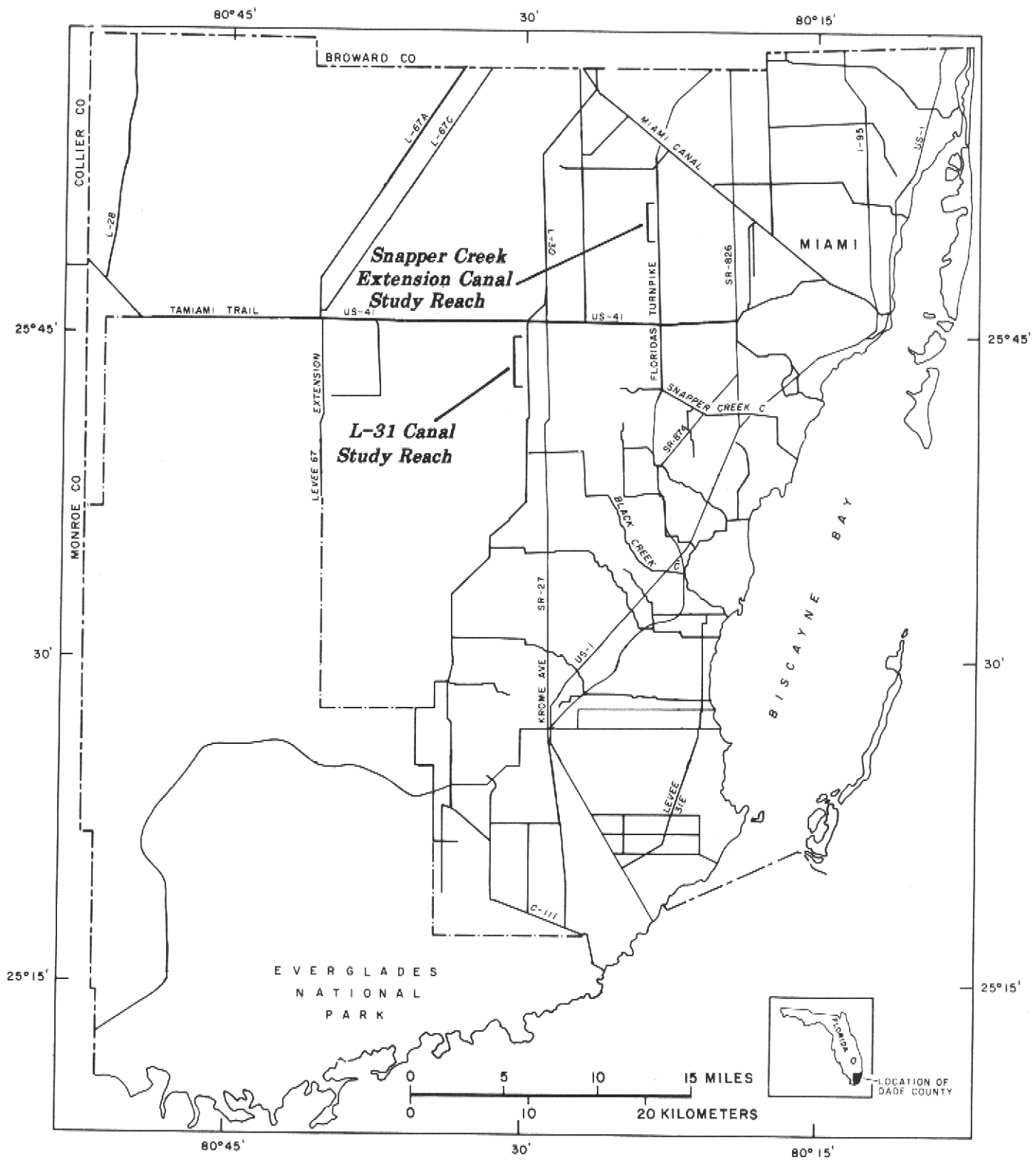
Figure 1. Location of L-31N and Snapper Creek Extension Canals.

The U.S. Geological Survey, in cooperation with the South Florida Water Management District and the Metro-Dade Department of Environmental Resources Management, conducted a study that involved UVM measurements for determination of discharge in the L-31N and Snapper Creek Extension Canals. The necessity of accurate discharge measurements required that the significance of side-friction effects for various width-to-depth ratios and sideslopes be examined. Average velocity calculations based on the 2-D equation were compared with those based on the standard 1-D method, and the results are presented in this report.

Purpose and Scope

This report explores the differences in calculating average cross-sectional velocity from measured line velocity when the 1-D von Karman velocity profile is replaced by an equation that represents both vertical and horizontal effects of boundary friction. The relation between mean and line velocity derived from this equation, referred to as 2-D, is compared with the standard relation based on the 1-D von Karman velocity profile, which accounts for boundary friction effects only in the vertical direction. These two formulations are compared for the cross sections at the L-31N Canal and Snapper Creek Extension Canal and for various other channel geometries to evaluate the significance of the differences in these schemes on velocity determinations.

Physical Setting of Study Sites

The L-31N Canal (fig. 1) has, at the study site, a bank elevation about 8 ft above sea level, a channel bed elevation 13 ft below sea level, and a regulated canal stage about 5.0 ft above sea level. The bottom of the canal has an 18-in. thick sediment layer with a hydraulic conductivity of 0.03 ft/d (Chin, 1990). This layer is not present on the channel sides, and the canal penetrates the Biscayne aquifer, which has a much higher hydraulic conductivity that varies from 5,000 to 40,000 ft/d. Aquatic growth on the bed and sides of the canal is minimal, and the section chosen for study is relatively straight and does not have bends and turns that would disrupt the flow patterns. The width-to-depth ratio is about 6.3:1.

The Snapper Creek Extension Canal (fig. 1) has a bank elevation 5 ft above sea level and a bed elevation that ranges from 13 to 28 ft below sea level. The canal stage is maintained near 0.5 ft above sea level. As is the case with the L-31N Canal, the Snapper Creek Extension Canal has a sediment layer on the bottom and penetrates the Biscayne aquifer. Aquatic growth is somewhat more prevalent there than at L-31N, but not excessive. Very low flow velocities exist in the Snapper Creek Extension Canal. This canal is about 3 mi east of the Northwest Well Field and is hydraulically connected with the shallow ground-water system. The width-to-depth ratio is about 2.9:1.

Ultrasonic Velocity Meter Method

The UVM method is generally accepted for measurement of low streamflow velocities (Gupta, 1989; Laenen and Curtis, 1989). The UVM operates on the basis that point-to-point traveltime of an acoustic signal is greater when the signal is traveling upstream than when it is traveling downstream. The difference in traveltime is due to the motion of the water relative to the transducers. Whereas streamflow measurements made with a mechanical current meter involve velocity measurements at many points across the channel cross section and can take 30 minutes or more, with the UVM, only a fraction of a second is required for the acoustic signal to pass across the channel. Thus, the UVM is much closer to being an instantaneous velocity measurement. In addition, the acoustic signal does not disrupt the flow patterns as a submerged mechanical current meter would, nor is meter motion a problem, as it could be for a suspended mechanical current meter.

Principles of Signal Travel

The acoustic signal of a UVM travels along a path set at an angle of 30 to 60 degrees to the flow; thus, the entire velocity profile in the horizontal between transducers is covered. Two such acoustic paths are shown, in plan view, in figure 2. The ultrasonic transducer is triggered by a single spike of excitation voltage and emits an acoustic pulse. When the acoustic pulse is received by the other transducer, it is transformed back into an electronic signal and the elapsed traveltime is measured. The same measurement is made in both directions, and the line velocity is determined using the following equation (Laenen, 1985):

$$u_L = \frac{B}{2 \cos \Theta} \left[\frac{1}{t_{dn}} - \frac{1}{t_{up}} \right], \qquad (1)$$

where u_L is average velocity measured along the acoustic path, B is length of acoustic path, Θ is angle between streamflow and acoustic path, t_{dn} is downstream traveltime, and t_{up} is upstream traveltime.

The velocity of the water is measured along the acoustic path. Because the path is set at an angle to the flow, cross currents can cause errors in measurement. For this reason, a standard approach is to set up two paths: one from left to right upstream and the other from right to left upstream (fig. 2). The two velocities obtained are averaged. When one acoustic path is used, an accuracy of ±3 percent can be attained; when a double path is used, ±1 percent accuracy is possible (Laenen, 1985).

Error Sources

There are several possible sources of error in the UVM method. The bending of the acoustic beam from temperature gradients, salinity gradients, and reflections from boundaries
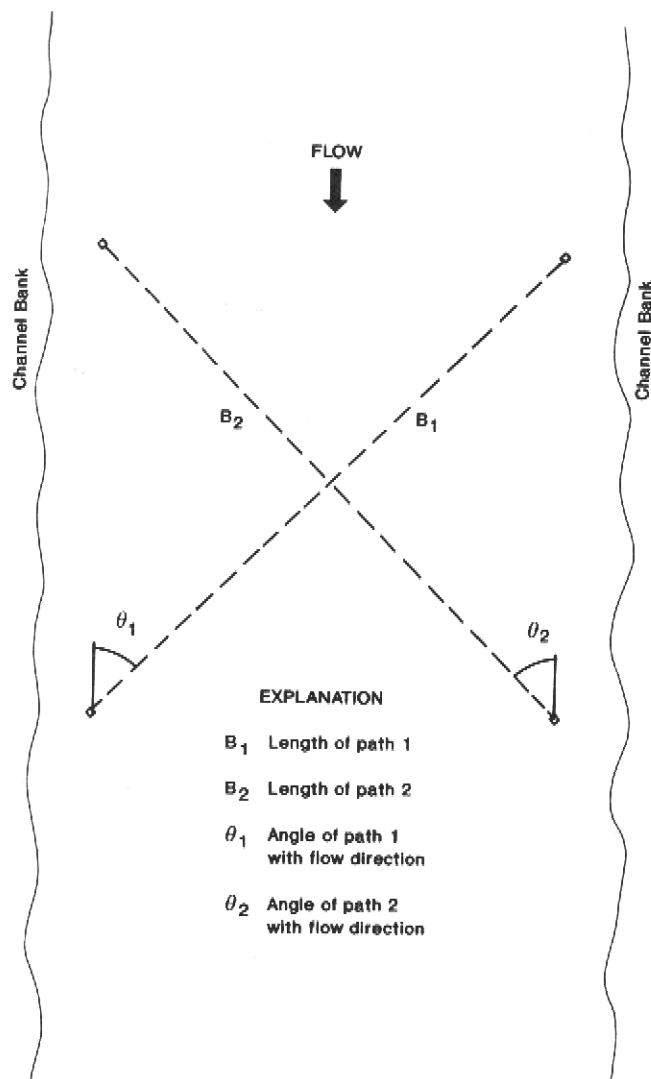
Figure 2. Acoustic path orientation.

EXPLANATION

B_1 Length of path 1

B_2 Length of path 2

θ_1 Angle of path 1 with flow direction

θ_2 Angle of path 2 with flow direction

FLOW

Channel Bank

Channel Bank

across the cross section, and the percentage of discharge outside the transducers can be calculated. This percentage can be added to future UVM measurements to account for these discharges. The parts of the cross section outside the transducers are in low velocity areas; thus, the percentage of discharge in these areas tends to be small.

LABORATORY AND FIELD TESTS OF THE ULTRASONIC VELOCITY METER

The accuracy of the UVM has been verified by tow-tank tests at the U.S. Geological Survey hydraulic laboratory. Velocity errors measured in these tests averaged 0.185 in/s over a path length of 15.4 ft. The accuracy increases for longer path lengths. In the tow-tank tests, velocity errors were actually 25 to 40 percent of the values predicted by theory (Laenen and Curtis, 1989).

The U.S. Geological Survey study (Chin, 1990) to measure leakage quantities in the L-31N and Snapper Creek Extension Canals (fig. 1) afforded an opportunity to use the UVM in the field. Stream velocities were measured at three locations along the L-31N Canal and at two locations along the Snapper Creek Extension Canal, at 1-mi intervals, to determine discharges. The differences in discharges were indicative of the leakage quantities. The leakage values determined from the differences in discharge measured at 1-mi intervals were on the order of 7 percent of the total canal flow, indicating the necessity that determination of average velocity from measured velocities be done precisely.

EFFECTS OF HORIZONTAL VELOCITY VARIATIONS

To correctly calculate the discharge from velocity and the cross-sectional area, average velocity must be ascertained; that is, the velocity integrated over the entire cross-sectional area, divided by the total area:

$$\bar{u} = \frac{\int_A v\ dA}{A}, \qquad (2)$$

where u is average velocity, A is cross-sectional area, and v is downstream velocity at each point in the cross section.

When using the UVM, downstream velocities are sampled at every point along the acoustic path. This is the "line velocity." Thus, integration in the horizontal direction is achieved by the diagonal path crossing the channel (fig. 2). The UVM measures:

$$u_L = \frac{\int_w v_p\ dw}{w}, \qquad (3)$$

where u_L is the line velocity, w is width of channel between transducers, and v_p is the downstream velocity at each point along the acoustic path. Thus, a way to convert u_L measured by the UVM to $\bar{u}$ to calculate discharge is needed.

can modify the effective path length or cause loss of signal (Falvey, 1983). Temperature gradients measured in the L-31N Canal and the Snapper Creek Extension Canal were determined to be negligible, salinity gradients were not significant, and boundary reflections did not interfere with the measurements. An oscilloscope was used to obtain a visual trace of the transmitted and received ultrasonic pulses, and reflected pulses were observed as secondary spikes. These almost always occurred after the main pulse was received. Uncertainties in measurement of path length and angle with streamflow are additional sources of error (Newman, 1982).

Perhaps the most significant source of error can be seen in the channel cross section and acoustic transducer locations shown in figure 3. Part of the cross section is always outside the acoustic path where velocity is not measured. Discharge in these regions must be estimated and added to the discharge component measured by the UVM. Point current meter velocity measurements can be made
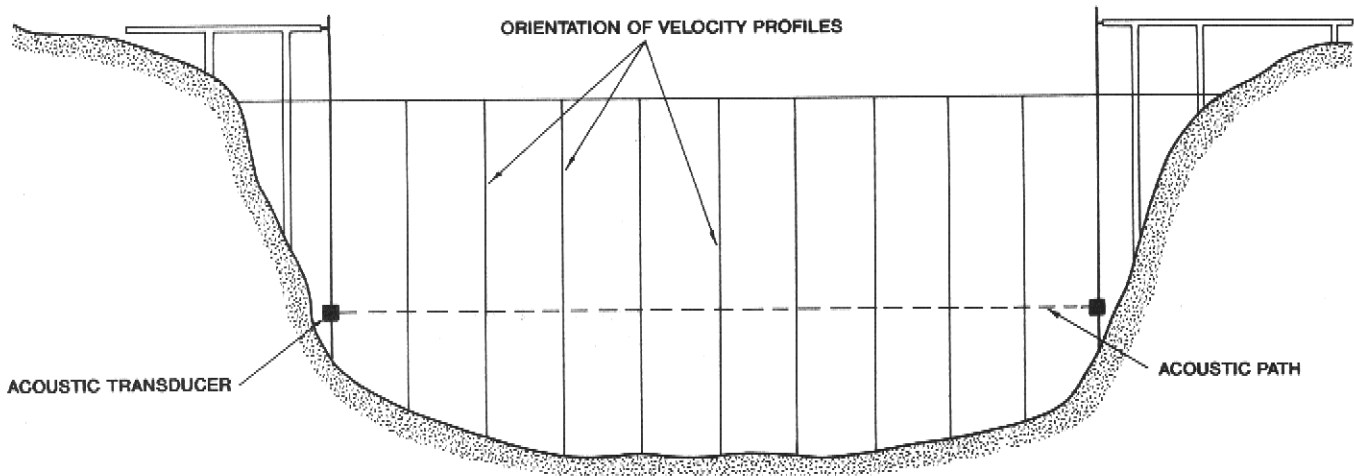
Figure 3. Channel cross section and one-dimensional orientation of velocity profiles.

The purpose of this exercise is to determine a coefficient K, which can be multiplied by the UVM-measured line velocity u_L to obtain the average velocity $\bar{u}$. Thus, K should be equal to the ratio $\bar{u}/u_L$ (W.G. Sikonia, U.S. Geological Survey, written commun., 1990).

The K coefficient can be determined by a polynomial curve fit between current meter measurements and corresponding UVM path velocities (Laenen, 1985). In this study, insufficient simultaneous current meter and UVM measurements were available for this curve fit, and a method based on an assumed velocity profile was necessary.

To compare u_L to $\bar{u}$, the relation of each individual v_p in equation 3 to the average velocity must be determined.

One-Dimensional Velocity Profile

If the assumption is made that the velocity at each location along the channel cross section varies in the vertical direction according to the von Karman universal velocity profile, then a direct relation between the measured velocity at any depth and the average velocity in the vertical is defined. Because the von Karman universal velocity profile defines only vertical variations in the downstream velocity, it can be referred to as the 1-D von Karman velocity profile. When determining average velocity from measured velocity, it is generally assumed that the vertical velocity profile follows the 1-D von Karman universal velocity profile (French, 1985, p. 29):

$$u = \frac{u_*}{k} \ln \frac{y}{y_0} = \bar{u} + \frac{u_*}{k} \left[1 + \ln \frac{y}{d} \right], \qquad (4)$$

where u is water velocity at distance y from bottom of channel, y_0 is the distance from the channel bottom to the point of zero velocity (boundary layer thickness), u_* is shear velocity, k is von Karman's constant = 0.41, and d is depth of water.

Manipulation of equation 4 gives:

$$u = \bar{u} \, a \, \ln \frac{by}{d} , \qquad (5)$$

where: $a = u_*/\bar{u}k$ and $b = d/y_0 = \exp(1 + k\bar{u}/u_*)$. Empirically determined values of $a = 0.1948$ and $b = 423.7$ are reported by Laenen (1985).

The channel cross section with acoustic transducer locations and vertical lines corresponding to the direction in which the 1-D von Karman profile defines variations in downstream velocity is shown in figure 3. These lines are the directions along which y and d are measured in equation 5. This equation applies when the solid (friction) boundary is at the bottom. Therefore, the 1-D von Karman profile is most accurate near the channel center; at the edges, the side friction modifies the profile.

Equation 5 leads to a formula for the correction factor K, which will correct the measured value to the average velocity, assuming that the velocity profile fits a 1-D von Karman distribution. The correction factor should relate the average velocity in the channel cross section to the line velocity measured along the acoustic path at a given elevation. If the channel cross section between the acoustic transducers is divided into vertical slices (fig. 3), the total flow between the transducers is the sum of the vertically averaged velocities in each slice times the area of each slice. Dividing by the total area between transducers gives the average velocity in this cross section:

$$\bar{u} = \frac{\displaystyle\sum_{i=1}^{n} \bar{u}_i A_i}{\displaystyle\sum_{i=1}^{n} A_i} = \frac{\displaystyle\sum_{i=1}^{n} \bar{u}_i A_i}{A} . \qquad (6)$$

Similarly, the line velocity measured by the UVM can be represented by a sum of point velocities along the line, weighted by the width corresponding to each point or:

$$u_L = \frac{\sum\limits_{i=1}^{n} u_i \, w_i}{\sum\limits_{i=1}^{n} w_i} = \frac{\sum\limits_{i=1}^{n} u_i \, w_i}{w} . \qquad (7)$$

Taking correction factor K equal to the ratio of average velocity to line velocity:

$$K = \frac{\bar{u}}{u_L} = \frac{w}{A} \frac{\sum\limits_{i=1}^{n} \bar{u}_i \, A_i}{\sum\limits_{i=1}^{n} u_i \, w_i} . \qquad (8)$$

However, if equation 5 is placed into the term u_i in the denominator of equation 8, a $\bar{u}_i$ term remains in both the numerator and denominator which cannot be canceled. This would require prior knowledge of $\bar{u}$ in each slice to calculate K. As a practical alternative to equation 8, Laenen (1985) presents an equation in which the ratio u_i/u_i is calculated for each slice and then area-weighted across the channel to obtain K. This equation is:

$$K = \frac{\sum\limits_{i=1}^{n} \frac{\bar{u}_i}{u_i} A_i}{\sum\limits_{i=1}^{n} A_i} = \frac{\sum\limits_{i=1}^{n} \left[\frac{A_i}{a \ln b y_i/d_i} \right]}{\sum\limits_{i=1}^{n} A_i} , \qquad (9)$$

where y is height of acoustic path above bottom at slice i, and d_i is water depth at slice i.

Equation 9 is based on the assumption (as previously described) that the 1-D von Karman profile applies at all points in the channel. The 1-D von Karman profile is not exact at the channel sides because of boundary friction; the wider the channel, the greater the width at the center where von Karman's profile is a good approximation. Also, using equation 9 instead of equation 8 involves the assumption that the ratio of average velocities is approximately equal to the average of the velocity ratios. This assumption seems more likely to be satisfied in wide channels of uniform depth than in narrower, more irregular cross sections.

Two-Dimensional Velocity Profile

Friction from the sides of a narrow channel may affect the evaluation of the velocity coefficient K. When considering the effects of channel sides, the velocity profile depends not only on the vertical distance from the channel bottom (fig. 3), but also on the distance from channel sides (Chiu and others, 1978). The lines along which the von Karman velocity profile applies tend to be approximately radial and meet the channel bed in a more perpendicular fashion as shown in figure 4. Because these lines have horizontal as well as vertical components, this velocity profile scheme is referred to as 2-D. Chiu and others (1976) postulated that the von Karman profile should be defined along a coordinate system representing the 2-D distribution as follows:

$$u = \frac{u_*}{k} \ln \frac{\varepsilon}{\varepsilon_0} , \qquad (10)$$
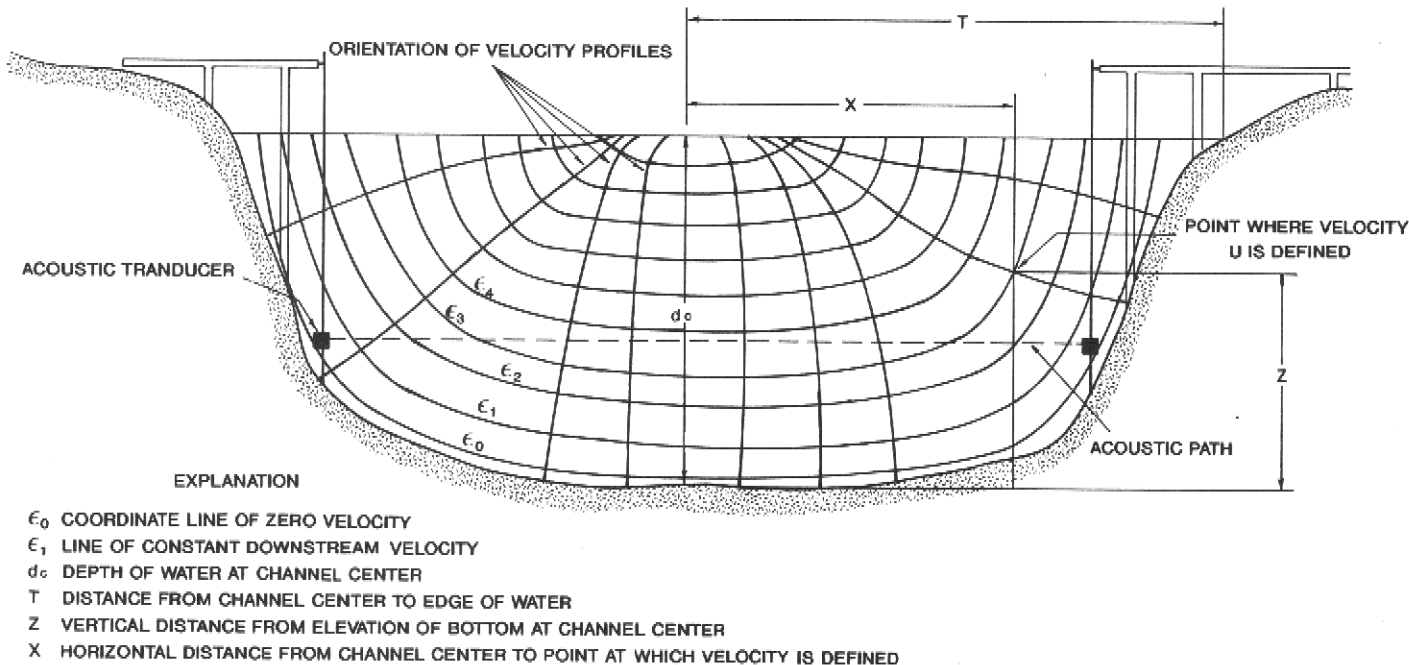
Figure 4. Channel cross section and two-dimensional orientation of velocity profiles.

EXPLANATION

ε_0 COORDINATE LINE OF ZERO VELOCITY
ε_1 LINE OF CONSTANT DOWNSTREAM VELOCITY
d_c DEPTH OF WATER AT CHANNEL CENTER
T DISTANCE FROM CHANNEL CENTER TO EDGE OF WATER
Z VERTICAL DISTANCE FROM ELEVATION OF BOTTOM AT CHANNEL CENTER
X HORIZONTAL DISTANCE FROM CHANNEL CENTER TO POINT AT WHICH VELOCITY IS DEFINED

where ε is an effective distance from the flow boundary, and ε_0 is a constant defining the flow boundary (point of effectively zero velocity). The lines of constant value of ε or, by equation 10, constant values of u, are shown in figure 4. These ε lines of constant downstream velocity are referred to as isovels. Because the von Karman velocity profile varies along the lines orthogonal to the ε lines, the velocity profile (defined by eq. 10) exists perpendicular to the isovel lines everywhere. For a natural channel, Chiu and others (1976) defined the isovel lines by:

$$u = \frac{z}{d_c}\left[1 - \frac{x}{T}\right]^\beta,\qquad(11)$$

where z is vertical distance from the elevation of the bottom at channel center, d_c is depth of water at channel center, x is the horizontal distance from channel center to the point at which the velocity is defined, T is distance from channel center to water edge, and β is a curve coefficient. This equation is an empirical curve fit to the isovel contours by a hyperbola. This equation applies to one-half the channel at a time (the T and x values defining the horizontal distance from the center as in fig. 4). Equation 11 indicates that the zero isovel line ($\varepsilon = \varepsilon_0$) is a distance $\varepsilon_0 d_c$ from the channel bed at the center of the cross section and a distance $T(\varepsilon_0)^{1/\beta}$ from the edge of water at the water surface. This distance between the channel bed and the point of zero velocity corresponds to a boundary layer, which also exists in the 1-D von Karman velocity profile (Daugherty and others, 1985, p. 220).

The coefficients β and ε_0 must be determined from the channel geometry and/or field velocities. Two methods exist for doing this. The first method is derived as follows. From equation 11, it can be seen that on the vertical axis at the channel center where $x = 0$,

$$\varepsilon = \frac{z}{d_c}.\qquad(12)$$

By combining equations 10 and 12:

$$u(z) = \frac{u_*}{k}\ln\frac{z}{d_c\varepsilon_0},\qquad(13)$$

where u(z) is the velocity at distance z above the bottom at the channel center. By rearranging equation 13:

$$\frac{u(z)}{\ln\left[\dfrac{z}{d_c\varepsilon_0}\right]} = \frac{u_*}{k}.\qquad(14)$$

Giving two different values of depth (z_1 and z_2) in equation 14, the expression obtained is:

$$\frac{u(z_1)}{\ln\left[\dfrac{z_1}{d_c\varepsilon_0}\right]} = \frac{u(z_2)}{\ln\left[\dfrac{z_2}{d_c\varepsilon_0}\right]}\qquad(15)$$

By rearrangement of terms:

$$[u(z_1) - u(z_2)]\ln\varepsilon_0 = u(z_1)\ln\frac{z_2}{d_c} - u(z_2)\ln\frac{z_1}{d_c}.\qquad(16)$$

Solving for ε_0:

$$\varepsilon_0 = \exp\left\{\frac{+\ln\left[\dfrac{z_1}{d_c}\right]\dfrac{u(z_2)}{u(z_1)} - \ln\left[\dfrac{z_2}{d_c}\right]}{\dfrac{u(z_2)}{u(z_1)} - 1}\right\}.\qquad(17)$$

Equation 17 gives ε_0 based on the ratio of velocities at two distances from channel bottom at the channel center. If the distances are chosen as $z_1 = 0.2d_c$ and $z_2 = 0.8d_c$, equation 17 becomes (French, 1985):

$$\varepsilon_0 = \exp\left\{\frac{0.22 - 1.61\left[\dfrac{u(0.8d_c)}{u(0.2d_c)}\right]}{\dfrac{u(0.8d_c)}{u(0.2d_c)} - 1}\right\}.\qquad(18)$$

The parameter β now can be determined from the cross-sectional area. For the half channel from center to the edge of the water, the cross-sectional area (A_H) is defined by:

$$A_H = \int_0^{T'}\int_{d_cf(x)}^{d_c} dz\,dx = \int_0^{T'}d_c - d_c\varepsilon_0\left[1 - \frac{x}{T}\right]^{-\beta} dx,\qquad(19)$$

where $f(x) = \varepsilon_0(1 - x/T)^{-\beta}$ and $T' = T(1 - (\varepsilon_0)^{1/\beta})$. (Note that $d_cf(x)$ is the height of the zero-velocity isovel above the elevation of the channel bottom at center of channel.) With a change of variable, $\zeta = 1 - x/T$ and $dx = -T\,d\zeta$ (Chiu and others, 1976),

$$A_H = \int_1^{(\varepsilon_0)^{1/\beta}}\left[d_c - d_c\varepsilon_0(\zeta)^{-\beta}\right](-T)\,d\zeta$$

$$= d_cT\left[1 - \frac{1}{1-\beta}\left(\varepsilon_0 - \beta\varepsilon_0^{1/\beta}\right)\right].\qquad(20)$$

Manipulating equation 20, the expression for β is:

$$\beta = 1 - \frac{\varepsilon_0 - \beta\varepsilon_0^{1/\beta}}{1 - \dfrac{A_H}{d_cT}}\qquad(21)$$

Equation 21 must be solved iteratively for β, knowing A_H, d_c, T, and ε_0 from equation 18.

The second method for determining β and ε_0 would apply if u(0.8d) and u(0.2d) were not known. Chiu and others (1976) derived the expression for average velocity over the entire half-channel cross section. Their results are:

$$\bar{u}_H = \frac{T\,d_c}{A_H}\frac{u_*}{k}\left(-1 - \beta - \ln\varepsilon_0 + \frac{\varepsilon_0 - \beta^2(\varepsilon_0)^{1/\beta}}{1 - \beta}\right).\qquad(22)$$

where $\bar{u}_H$ is the average velocity in the entire half channel.

Because $\dfrac{u_*}{u_H} = \sqrt{\dfrac{f}{8}} = \dfrac{n\sqrt{g}}{c R^{1/6}}$, where n is Manning's friction factor, f is the Darcy-Weisbach friction factor, c is 1 in System International units and 1.49 in foot-pound units, g is gravitational acceleration, and R is hydraulic radius, this can be put in the form:

$$\frac{T d_c}{A_H k} \frac{n\sqrt{g}}{c R^{1/6}} \left(-1 - \beta - \ln \varepsilon_0 + \frac{\varepsilon_0 - \beta^2 (\varepsilon_0)^{1/\beta}}{1 - \beta} \right) - 1 = 0. \quad (23)$$

Knowing T, d_c, A_H, n, and R, equations 20 and 23 can be solved simultaneously to obtain β and ε_0. Because an iterative solution is necessary in two unknowns, a Newton-Raphson iterative solution can be used to solve these equations.

Using either of these methods requires knowing A_H, d_c, and T. The first method can be used if good field values of u(0.8d) and u(0.2d) exist. The second method can be used if values of n and R are known for the canal and cross section.

The method of representing isovel curves by the hyperbolic equation 11 cannot be expected to match the profile in all cross-sectional shapes. The two methods described are attempts to calculate ε_0 and β coefficients that create isovels based on measured velocities and channel dimensions. There are several anomalies in this method that create isovel shapes deviating from what would be expected. One common location for a deviation is at the channel side where the zero isovel encompassed an area equal to the cross-sectional area, but is not the same shape as the actual channel side. Another deviation occurs at the channel center where the slopes of the isovel lines are not horizontal as expected.

Rearranging equation 11 and taking a derivative gives:

$$\frac{\partial z}{\partial x} = \frac{\beta \varepsilon d_c}{T} \left(1 - \frac{x}{T} \right)^{-\beta - 1} \quad (24)$$

Thus, at the channel center, the isovel slope $\dfrac{\partial z}{\partial x} = \dfrac{\beta \varepsilon d_c}{T}$.

Near the channel bed, ε is small and the slope is small. However, near the water surface, the slope at channel center can be significantly large (fig. 6, shown later in the report). This would tend to show a "point" on the bottom of the isovel curve if the entire channel (both halves) were portrayed. This "point" should be smoothed out to be more realistic and appear as in figure 4. A similar "point" is seen in the 1-D von Karman profile (Daugherty and others, 1985, p. 220).

These anomalies can create errors when equation 11 is used, but the purpose of this report is to explore the differences in the 1-D and 2-D approaches to calculating average velocity, not to create a precise 2-D equation. Thus, equation 11 is sufficient for the purposes of defining a 2-D profile for basic comparison with the 1-D assumptions.

The 2-D velocity profile, defined by equations 10 and 11, can be used to create a K coefficient as was the 1-D profile used to create equation 9. In portraying the half-channel case, equations 10 and 11 can be combined as:

$$u = \frac{u_*}{k} \ln \left[\frac{1}{\varepsilon_0} \left(\frac{z}{d_c} \right) \left(1 - \frac{x}{T} \right)^{\beta} \right] = \frac{u_*}{k} \ln \left[\frac{z}{d_c f(x)} \right], \quad (25)$$

where $f(x) = \varepsilon_0 (1 - x/T)^{-\beta}$, and where $d_c f(x)$ is the height of the zero-velocity isovel above the centerline channel bottom.

The discharge per unit width at a distance x from the centerline of the channel, q(x), can be found by vertically integrating the velocity in equation 25:

$$q(x) = \int_{d_c f(x)}^{d_c} u\, dz = \int_{d_c f(x)}^{d_c} \frac{u_*}{k} \ln \left(\frac{z}{d_c f(x)} \right) dz, \quad (26)$$

Performing the integration yields:

$$q(x) = \frac{u_*}{k} d_c \left[-\ln f(x) + f(x) - 1 \right] \quad (27)$$

To obtain $\bar{u}$ for the entire cross section, equation 27 integrated over the cross-section width. This gives the form:

$$\bar{u} = \frac{1}{A_T} \int_{0}^{T-T_{DEOW}} q(x) dx - \frac{u_* d_c}{A_T k} \int_{0}^{T-T_{DEOW}} \left[-\ln f(x) + f(x) - 1 \right] dx, \quad (28)$$

where A_T is the cross-sectional area from channel center to acoustic transducer, and T_{DEOW} is the distance of the transducer from the edge of the water. It would not be possible to evaluate this integral in the 1-D case because the profile is not defined in the horizontal direction.

Performing a change of variables with $\zeta = 1 - x/T$ and $dx = -T\, d\zeta$, equation 28 becomes:

$$\bar{u} = \frac{u_* T d_c}{k A_T} \int_{1}^{T_R} \left[\ln \varepsilon_0 \zeta^{-\beta} - \varepsilon_0 \zeta^{-\beta} + 1 \right] d\zeta, \quad (29)$$

where T_R is T_{DEOW}/T. Performing the integration in equation 29 and simplifying yields:

$$\bar{u} + \frac{u_* d_c T}{k A_T} \left[(T_R - 1)(\ln \varepsilon_0 + \beta + 1) + \left(T_R^{1-\beta} - 1 \right) \frac{\varepsilon_0}{\beta - 1} - \beta T_R \ln T_R \right]. \quad (30)$$

The area A_T in equation 30 can be expressed by the integral:

$$A_T = \int_{0}^{T-T_{DEOW}} \int_{d_c f(x)}^{d_c} dz\, dx = \int_{0}^{T-T_{DEOW}} \left[d_c - d_c \varepsilon_0 \left(1 - \frac{x}{T} \right)^{-\beta} \right] dx. \quad (31)$$

Evaluating this integral yields:

$$A_t = T d_c \left[\frac{\varepsilon_0}{\beta - 1} \left(1 - T_R^{1-\beta} \right) - T_R + 1 \right] \quad (32)$$

Substituting equation 32 into equation 30 and simplifying yields:

$$\bar{u} = \frac{u_*}{k} \frac{(T_R-1)(\ln \varepsilon_0 + \beta + 1) + \left(T_R^{1-\beta} - 1\right)\dfrac{\varepsilon_0}{\beta-1} - \beta T_R \ln T_R}{\dfrac{\varepsilon_0}{\beta-1}\left(1 - T_R^{1-\beta}\right) - T_R + 1}. \quad (33)$$

The derivation of the line velocity from the 2-D equation is a form similar to equation 3:

$$u_L = \frac{1}{T-T_{DEOW}} \int_0^{T-T_{DEOW}} u_*/k \ \ln\left(\frac{z_T}{d_c} \frac{1}{f(x)}\right) dx, \quad (34)$$

where z_T is the vertical distance from the channel bottom in the center to the level of the acoustic transducer path. The integration yields:

$$u_L = \frac{u_*}{k}\left[\ln \frac{z_T}{\varepsilon_0 d_c} + \beta\left(\frac{\ln T_R}{1-(1/T_R)} - 1\right)\right]. \quad (35)$$

If equations 33 and 35 are put into equation 8, the following is obtained for the 2-D case:

$$K_{2D} = \frac{(T_R - 1)(\ln \varepsilon_0 + \beta + 1) + \left(T_R^{1-\beta} - 1\right)\dfrac{\varepsilon_0}{\beta-1} - \beta T_R \ln T_R}{\left[\dfrac{\varepsilon_0}{\beta-1}\left(1 - T_R^{1-\beta}\right) - T_R + 1\right]\left[\ln \dfrac{z_T}{\varepsilon_0 d_c} + \beta\left(\dfrac{\ln T_R}{1-(1/T_R)} - 1\right)\right]}. \quad (36)$$

The input variables T_R, z_T, and d_c can all be measured in the field.

After obtaining β and ε_0, by either of the two methods described above, equation 36 gives the 2-D K coefficient for the one-half channel modeled by β and ε_0. If the channel is symmetric, this can be considered the K value for the entire channel. If not, this procedure is repeated for the other half of the channel.

Certain limitations apply to equation 36 and to the 1-D equation 9 because of the assumption that the velocity profile is affected only by boundary friction. If wind-driven flows are significant in magnitude relative to the mean flow, the velocity profile can be distorted from that predicted by von Karman's equation. If the mean flow velocity is low, eddy velocities can become significant and alter the velocity profile. Profuse aquatic growth can make the position of the channel boundary difficult to define and the equation difficult to apply. In these cases, it is desirable to supplement any prediction of velocity profile with actual measurements, if possible.

K Value Comparison for Hypothetical Channels

To evaluate the differences quantitatively between the 1-D and 2-D equations for calculating the K coefficient, both equations were compared for theoretical channel cross

sections. A trapezoidal cross section was chosen, and differing width-to-depth ratios, sideslopes, and transducer depths were simulated.

For purposes of comparison, the parameters used in the 1-D and 2-D equations should be the same. In the 1-D equation 9, the channel geometry is specified by points along the riverbed. The trapezoidal cross section requires only three vertical panels to define the cross section for the 1-D equation 9. The values in equation 9 of a = 0.1948 and b = 423.7 for many natural channels (Laenen, 1985) were used to express the frictional effects in the 1-D equation. This does not correspond exactly to a single value of n for the 2-D equation 23. Comparing equations 4 and 5 with $u_*/u = \sqrt{f/8}$, the value of a = 0.1948 requires f = 0.05103, and the value b = 423.7 requires f = 0.05275. In equation 23, a value f = 0.0519 was used as the closest approximation. This corresponds to a Manning's n of 0.030 in a 10-ft deep, wide channel. Equations 20 and 23 were then solved simultaneously to obtain β and ε_0 (method 2). In the 2-D equation 36, the channel geometry is defined by the top width, depth at center, and half-area between the transducers. It should be noted that when equations 20 and 23 are used to calculate β and ε_0, the total half-channel cross-sectional area A_H is used.

The transducer depth and distance from the edge of the water must, of course, be specified the same in both equations, as well as identical depths of water. Because this is a symmetric channel, the K for the half channel calculated by equation 36 applies to the entire channel.

The first point of interest is how reasonable the 2-D equation is in predicting the isovels in the channels. A plot of the isovels, using β and ε_0 values produced by equations 20 and 23 for a trapezoidal channel with sideslope 2:1 and width-to-depth ratio of 6:1, is shown in figure 5. The zero isovel tends to curve outside and back into the cross section at the channel side. A similar phenomenon was reported by Chiu and others (1976). This is a result of the hyperbolic curve fitting in the original equation 11. It cannot always exactly match a channel shape. However, the isovels of interest in equation 36 are not those outside the area between the transducers, and errors in fitting the channel boundary will be concentrated at the sides.

The hypothetical trapezoidal channel was analyzed for several configurations. First, the sideslope was fixed at two vertical to one horizontal, the transducer was fixed at a position 4 ft above the channel bed (6-ft deep and 3 ft from edge of water), and the width-to-depth ratio for the entire channel (not the half cross section) was varied from 3:1 to 20:1. The relation between the resulting K values and the width-to-depth ratio are shown in figure 6. The sideslope was changed to 1:1 and the K values shown in figure 7. Finally, the transducer depth was raised to 5 ft below surface and the K values shown in figure 8. Note that transducer depth is defined in the illustrations as distance from the water surface, according to U.S. Geological Survey convention.
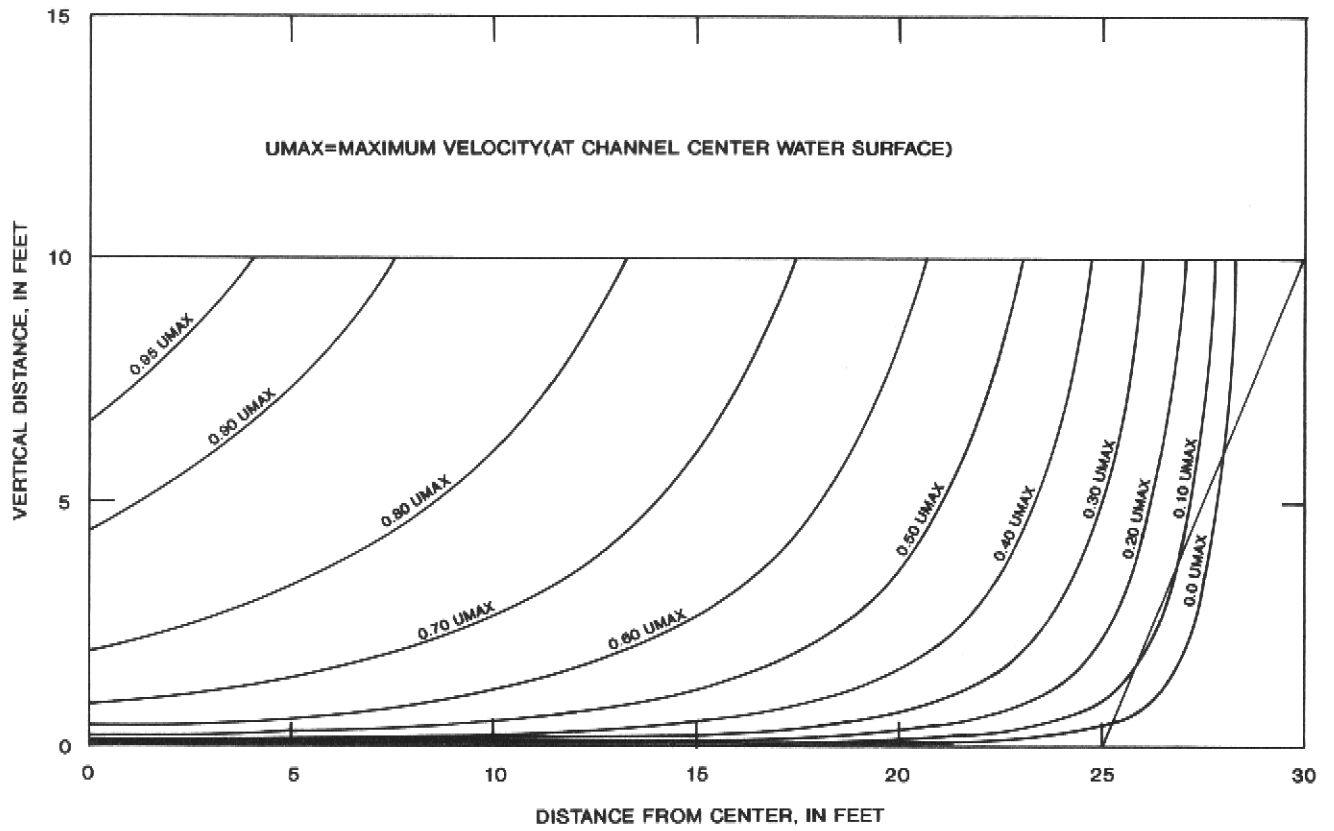
Figure 5. Lines of equal velocity for a trapezoidal channel calculated from two-dimensional equation.

Figure 6. Relation between K coefficient and width-to-depth ratio for sideslope 2:1 and transducer at 0.6 depth.

Figure 7. Relation between K coefficient and width-to-depth ratio for sideslope 1:1 and transducer at 0.6 depth.

Figure 8. Relation between K coefficient and width-to-depth ratio for sideslope 1:1 and transducer at 0.5 depth.

Figure 9. Lines of equal velocity for L-31N mile 1 cross section calculated from two-dimensional equation.
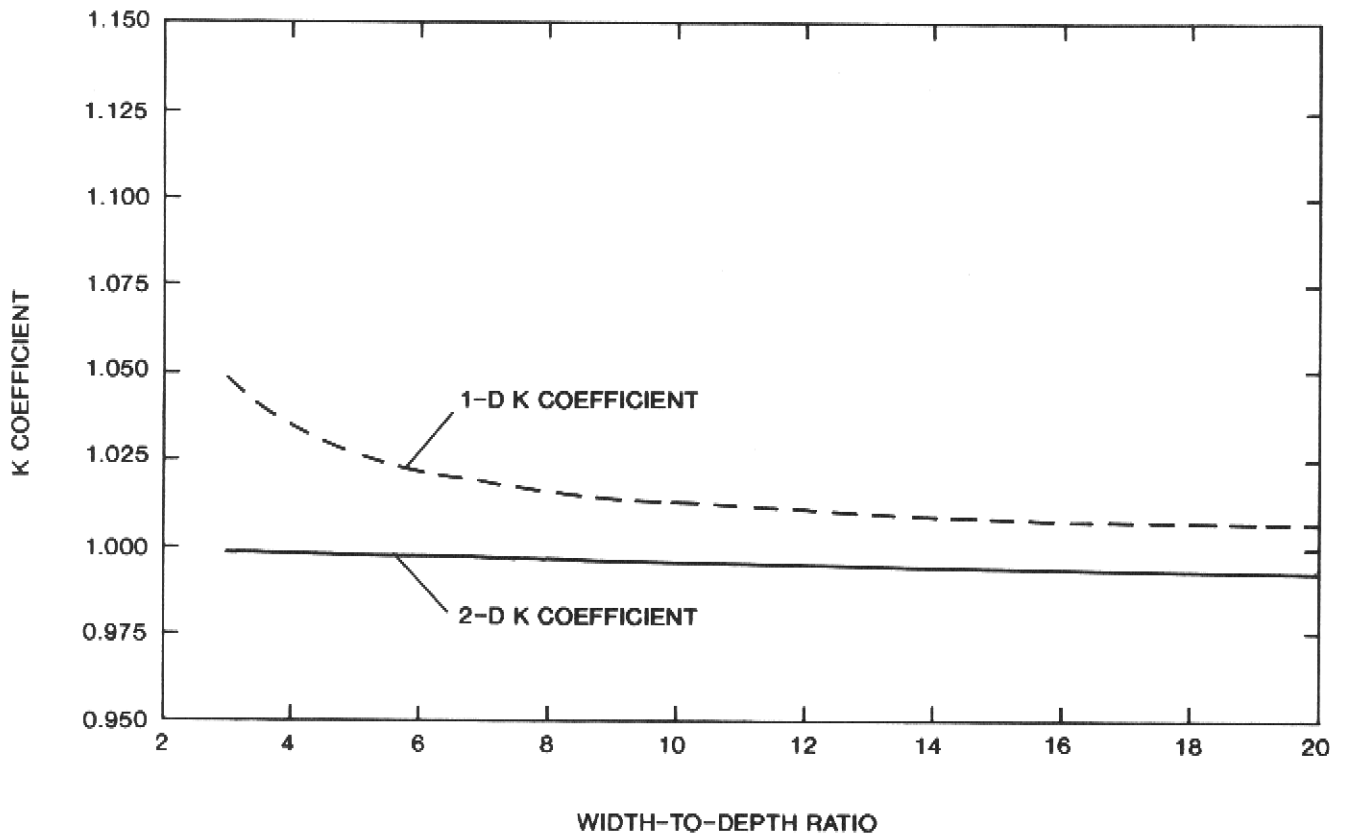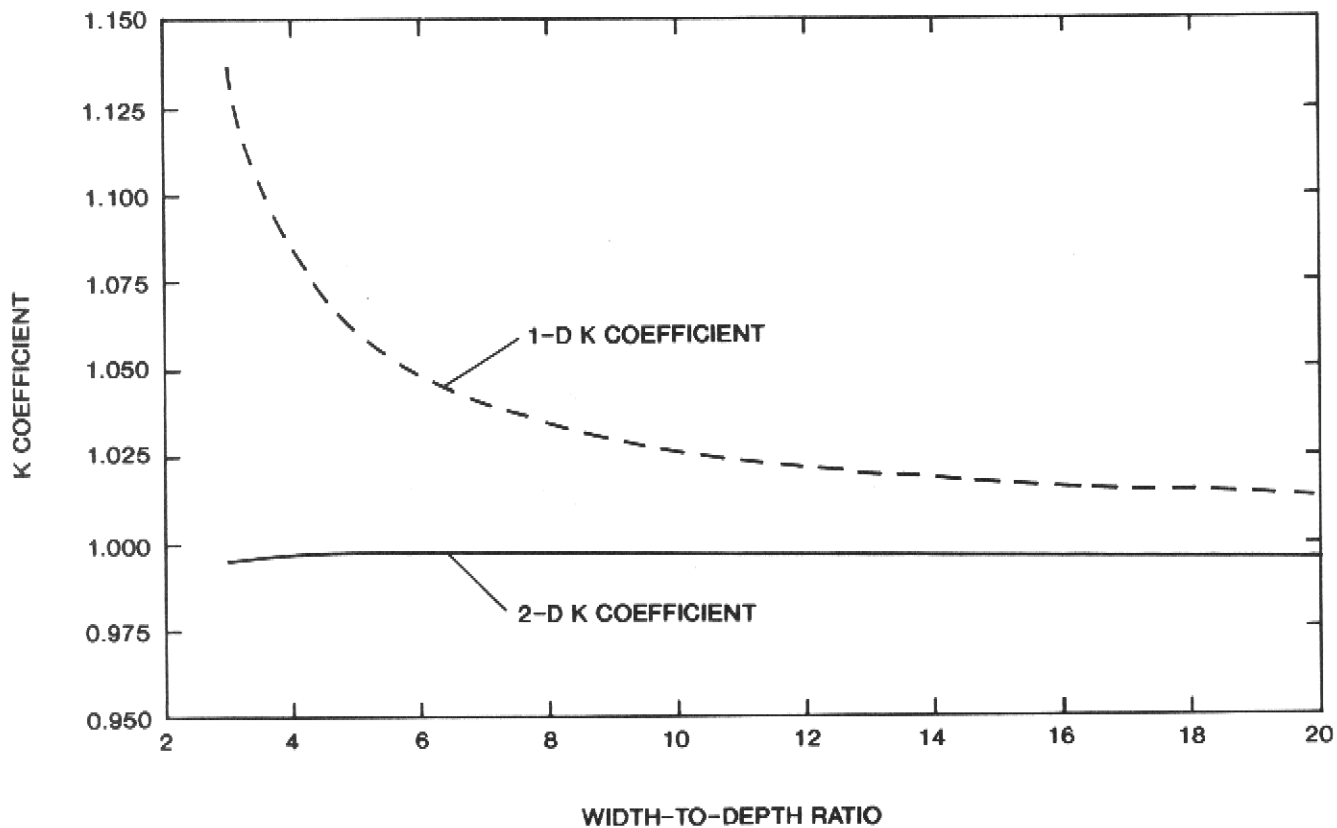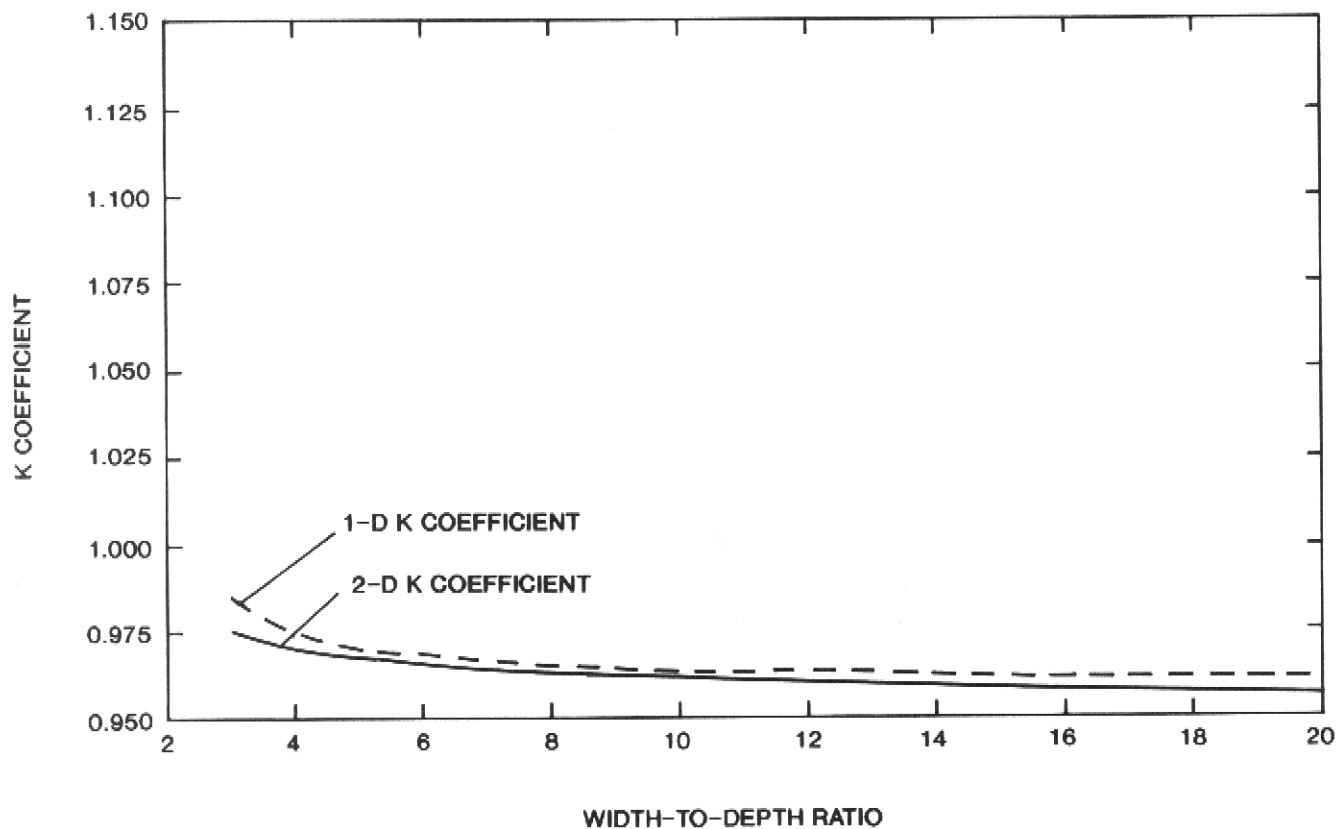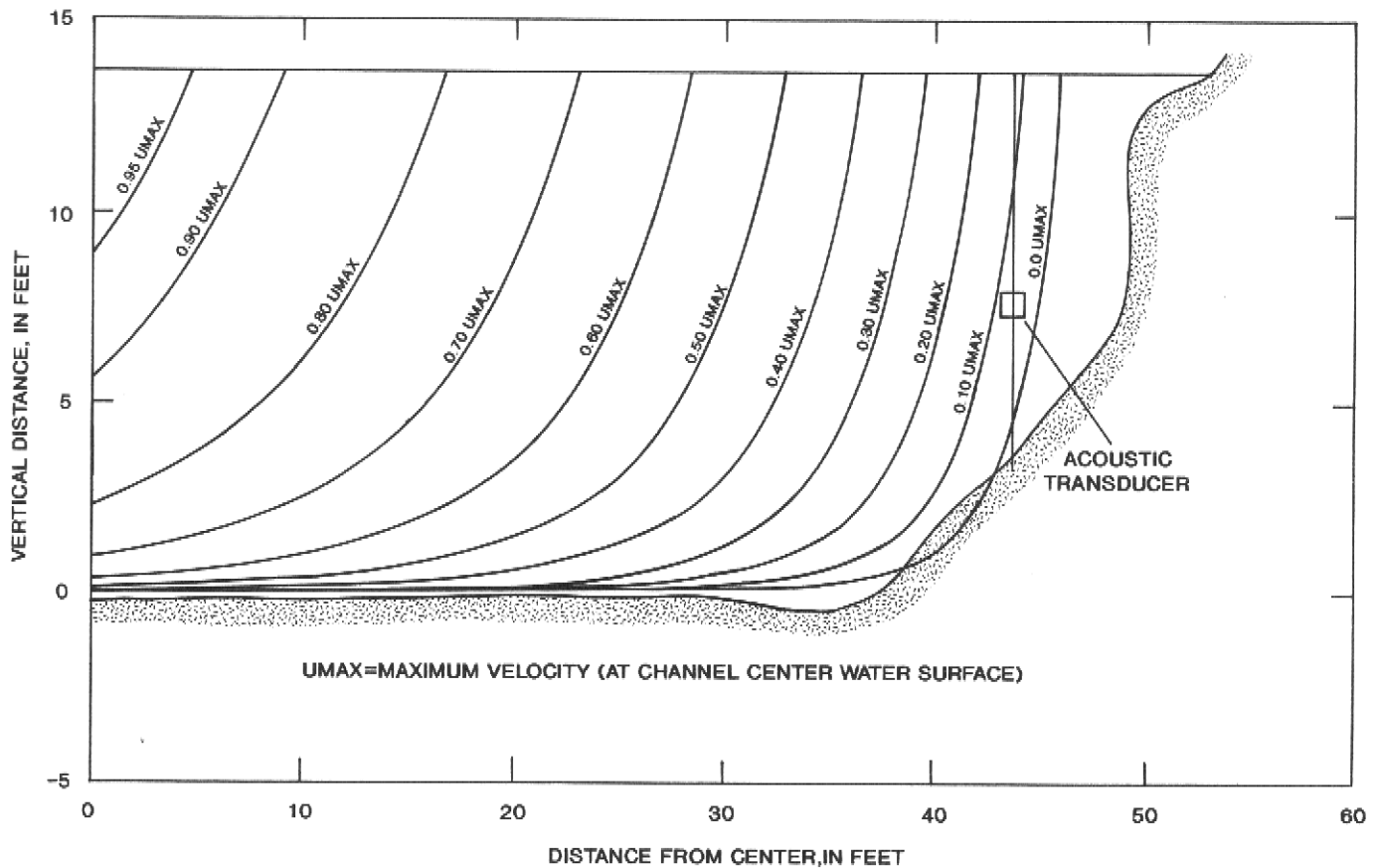
In the channel configurations shown in figure 6, the 2-D parameters varied from $\beta = 4.283$ $\varepsilon_o = 0.000149$ at a width-to-depth ratio of 3:1 to values of $\beta = 1.650$ $\varepsilon_o = 0.000515$ at a width-to-depth ratio of 20:1. In the cross sections of figures 7 and 8, the parameters varied from $\beta = 8.244$ $\varepsilon_o = 0.0000439$ at a width-to-depth ratio of 3:1 to $\beta = 2.2567$ $\varepsilon_o = 0.0003127$ at a width-to-depth ratio of 20:1.

The most unexpected result seen in figures 6 to 8 is the insensitivity of the 2-D K coefficient to the width-to-depth ratio. As low width-to-depth ratio (narrower, deeper channel) conditions are approached, the 1-D K coefficient increases exponentially, whereas the 2-D K coefficient only displays a slight increase. A slight decrease is even observed in the 2-D K at low width-to-depth ratios in figure 7. These trends are consistent to varying degrees in figures 6 to 8, indicating that this behavior exists for different channel sideslopes and transducer depths. An examination of the velocity profiles may explain the behavior of both K coefficients.

Equations 8 and 9 indicate that, when the points where the velocity is measured (location of acoustic path) are proportionately lower on the 1-D vertical velocity profile, values of u/u_L are higher. Figure 3 shows this occurring near the sides of the channel, and equation 8 indicates higher values of $\bar{u}/u_L$ corresponding to a higher overall 1-D K for all the vertical

slices. For a trapezoidal channel, narrowing the channel while maintaining the same sideslope is equivalent to reducing the area in the channel center, making the side areas more dominant in their contribution to the 1-D K. This exponential increase in the 1-D K (figs. 6-8) can be expected from the equations when the channel is made narrower. However, the 2-D equation 36 accounts for horizontal friction effects on average velocity when calculating the 2-D K. Therefore, as the channel is made narrower, side-friction effects project farther toward the channel center. These effects are seen graphically by the upward curves of the ε lines near the channel sides in figure 4. Thus, as the channel is made narrower, line velocities (u_L) become lower, but also lower values of average velocity ($\bar{u}$) for the entire cross section are generated by the 2-D calculations. With both u_L and u undergoing similar reduction as the channel is made narrower, the 2-D K = $\bar{u}/u_L$ does not seem to change much. This may be a more accurate depiction of the situation than is seen in the K_{1D} values. It can be concluded, therefore, from figures 6 to 8 and from the preceding argument, that the higher values of K_{1D} seen for channels with a low width-to-depth ratio are probably not an exact depiction of the actual situation, but are rather caused by lack of consideration in the 1-D solution of horizontal frictional effects and resulting velocity variations.

Table 1. Comparison of one- and two-dimensional (1-D and 2-D) K coefficients at the L-31N Canal and the Snapper Creek Extension Canal sites

Location	1-D K coefficient	2-D K coefficient Method 1	2-D K coefficient Method 2	Percent difference Method 1/ method 2	Percent difference 1-D K/2-D K (method 2)
		L-31N Canal			
Mile 1	0.963	0.9692	0.9598	+1.0	+0.3
Mile 2	.994	.9787	.9795	- .1	+1.5
Mile 3	.962	.9746	.9571	+1.8	+ .5
		Snapper Creek Extension Canal			
South	.896	---	.9325	—	-3.9
North	.934	—	.9831	—	-5.0

As would be expected from the argument presented in the previous paragraph, the K_{1D} and K_{2D} values are much closer in channels with higher width-to-depth ratios (figs. 6-8). Differences between the two solutions at high width-to-depth ratios may be attributable to the following: (1) K_{1D} was not derived from the exact equation 8, but by the approximation equation 9; and (2) as evidenced by figure 5, the 2-D isovels defined by β and ε do not fit the channel geometry exactly. It does appear that the K_{1D} tends to be higher than K_{2D}, indicating that using a 1-D approximation results in a tendency to overestimate K in the cases examined here.

Comparison of figures 6 and 7 indicates that reducing the sideslope increases the 1-D K but changes the 2-D K insignificantly. Comparison of figures 7 and 8 shows that raising the transducer lowers both the 1-D and 2-D K, as would be expected.

K Value Comparison for Field Channels

To assess inaccuracies in K coefficient determination, the 1-D and 2-D equations were used to determine K values at three UVM sites in L-31N Canal and at two UVM sites in Snapper Creek Extension Canal. Accurate cross-sectional measurements were made, and some point velocity measurements were taken with a mechanical current meter and an acoustic point velocity meter. For the 1-D equation, the measured cross-sectional points and transducer depth were specified. In the 2-D equation, the measured cross sections were used to specify A_{II}, T, and d_c. The transducer location was specified, and the n values corresponding to the friction assumption in the 1-D equation were used. This yields Manning's n values of 0.033 in L-31N Canal and 0.035 in Snapper Creek Extension Canal. Because point velocity measurements were available at L-31N Canal sites, it was possible to calculate β and ε_o at these sites by method 1 using u(0.8d), u(0.2d) and by method 2 using n. The very low velocities in Snapper Creek Extension Canal (0.03 ft/s) made 0.8- and 0.2-depth velocity measurements infeasible, and only method 2 could be used.

The measured cross section for one half of the channel at L-31N Canal mile 1 (dotted line) is shown in figure 9. The box indicates the transducer location, and the solid lines are the isovel lines computed from the values of β and ε_o obtained from equations 20 and 23.

Results of the K coefficient analysis are given in table 1, and the parameters used in the 2-D equations for these field sites are given in table 2. In L-31N Canal, the values of K_{1D} were always higher than the values of K_{2D} calculated by method 2 (table 1) consistent with the results in the hypothetical channels. However, the values of K_{2D} calculated by method 1 at L-31N miles 1 and 3 are actually higher than their corresponding K_{1D} values. The differences between method 1 and method 2 were 1.0 and 1.8 percent at these sites, respectively, compared to 0.1 percent at mile 2. This would tend to indicate that the 0.8 and 0.2 depth measurements used in method 1 may not be accurate enough in determining the β and ε_o coefficients, at least at miles 1 and 3.

The tendency shown in the hypothetical channels of K_{1D} being larger than K_{2D} is contradicted in the Snapper Creek Extension Canal cases. However, a comparison of figures 7 and 8 indicates that, when the transducer is raised from 0.6 to 0.5 depth, the K_{2D} values are not as far below the K_{1D} values. Thus, it is not unexpected that, in a situation where the transducers are even higher, the K_{2D} values can be larger than K_{1D}. In Snapper Creek Extension Canal, the transducers are placed at 0.37 depth and 0.24 depth at the north and south stations, respectively. The transducers at the L-31N Canal sites are nearer to 0.5 depth, so the results there are more similar to the hypothetical channels in figures 6 to 8. This also indicates that the tendency for the 1-D method to estimate a higher K value is most likely when the transducers are lower in the channel cross sections.

The percent difference between K_{1D} and K_{2D} calculated by method 2 is listed in table 1. The greatest difference was 5.0 percent at Snapper Creek north station, and the smallest different was 0.3 percent at L-31N mile 1. Because Snapper Creek Extension Canal has a smaller width-to-depth ratio (2.9:1) than L-31N Canal (6.1), and the results from the hypothetical channels indicate that smaller width-to-depth

Table 2. Parameters used in calculating two-dimensional K at the L-31N Canal and the Snapper Creek Extension Canal sites [Stage in feet above sea level; d_c, z_T, T, and T_{DEOW} in feet; A_H and A_T in square feet; and u(0.2d) and u(0.8d) in feet per second]

Location	Stage	d_c	z_T	T	T_{DEOW}	A_H	A_T	u(0.2d)	u(0.8d)	Method 1		Method 2	
										β	ε_o	β	ε_o
							L-31N Canal						
Mile 1	4.60	15.3	7.76	55	12.00	689	621	0.587	0.650	7.954	4.107×10^{-7}	5.0081	1.07×10^{-4}
Mile 2	4.60	16.6	8.05	50.5	10.30	667	613	.547	.650	6.993	5.101×10^{-6}	5.2859	9.99×10^{-5}
Mile 3	4.60	16.8	8.24	54	13.75	770	675	.446	.489	7.972	9.671×10^{-8}	4.3399	1.29×10^{-4}
						Snapper Creek Extension Canal							
South	.90	32.4	24.53	40	6.75	1,010	952	—	—	—	—	5.2647	1.00×10^{-4}
North	.90	18.6	11.75	38	8.50	506	462	—	—	—	—	6.5556	7.65×10^{-5}

ratios correspond to greater differences in K_{1D} and K_{2D}, it was expected that Snapper Creek Extension Canal would have larger differences than L-31N Canal.

Considering that the UVM can be accurate to ± 1 percent (Laenen, 1985), it appears that calculating K with a 1-D assumption might cause substantial errors in UVM discharge measurements, such as in the Snapper Creek Extension Canal. However, differences between K_{2D} values calculated by methods 1 and 2 were greater than differences between K_{1D} and K_{2D} values at two L-31N Canal sites, indicating that errors in calculating β and ε_o, and the curve fit they define, may be greater in some circumstances than the errors caused by assuming a 1-D velocity profile. Thus, a more precise curve-fitting algorithm than that developed by Chiu and others (1976) may be needed before actually replacing the 1-D K coefficient equation with a 2-D equation.

As indicated in table 2, methods 1 and 2 produce quite different values of β and ε_o at the L-31N sites. However, in table 1, the K_{2D} values for the two methods differ by no more than 1.8 percent, and only have a 0.1 percent difference at mile 2, indicating that the value of K_{2D} is not very sensitive to the values of β and ε_o chosen. The selection of β and ε_o is perhaps the weakest part of the 2-D equation.

An acoustic point velocity meter (Neil Brown[1] meter) was used at the L-31N Canal site to determine discharge simultaneously with the UVM measurements. The channel cross section was divided into 20 or more vertical slices, and velocity measurements at 0.2 and 0.8 depth in each slice were made with the Neil Brown meter. The two measurements were averaged in each slice and multiplied by the slice area to obtain the discharge in each slice. The sum of these discharges is the total discharge.

The discharges calculated from the UVM measurements using the 1-D and 2-D K are compared with the discharge calculated from the Neil Brown point velocity measurements in table 3. In all cases, the UVM discharge calculated with the 2-D K is closer to the Neil Brown measurement than the discharge calculated with the 1-D K. However, both UVM discharge values seem to always be higher than the Neil Brown measurements, sometimes drastically, indicating the existence of additional factors causing variations between the UVM and Neil Brown measurements.

---

[1]Use of brand names in this report is for identification purposes only and does not constitute endorsement by the U.S. Geological Survey.

Table 3. Comparisons of discharge calculated from ultrasonic velocity measurements by one-dimensional and two-dimensional (1-D and 2-D) K coefficient equations and by Neil Brown meter point velocity measurements in the L-31N Canal

Date	Mile	Stage (feet, above sea level)	1-D K	2-D K	Discharge, in cubic feet per second			Percent difference	
					1-D K	2-D K	Neil Brown	1-D/Neil Brown	2-D/Neil Brown
3/27/89	1	4.63	0.964	0.960	767	764	737	4.1	3.7
	2	4.62	.994	.980	715	705	669	6.9	5.4
	3	4.62	.962	.957	720	716	596	20.8	20.1
3/29/89	3	4.60	.962	.957	675	671	629	7.3	6.7
4/3/89	1	4.65	.964	.960	786	783	638	23.2	22.7
	2	4.61	.994	.980	748	737	685	9.2	7.6
	3	4.61	.962	.957	635	632	577	10.1	9.5

SUMMARY AND CONCLUSIONS

To determine discharge in the Snapper Creek Extension and L-31N Canals near Miami, Fla., with an ultrasonic velocity meter (UVM), it was necessary to accurately determine average velocity in the channel. The standard method of correcting the measured velocity between transducers in the stream to average velocity for the stream is to use a correction factor K that only considers the effects of the channel boundary friction in the vertical direction (one dimensional, 1-D). However, the actual velocity profile is affected by boundary friction in both the vertical and horizontal directions (two dimensional, 2-D).

An equation was developed in an attempt to account for the 2-D variation in velocity caused by channel boundary friction. This new equation includes a more accurate representation of the ratio of average velocity to measured velocity than is used in the standard 1-D K equation. The 2-D K equation was compared to the standard 1-D K equation for theoretical channel cross sections of varying width-to-depth ratios, sideslopes, and UVM transducer locations. The comparison indicates that the 1-D K and 2-D K deviate the most for narrower deeper channels. This is consistent with the fact that side-friction effects create a horizontal velocity variation not incorporated in the 1-D equation.

Comparison of the two methods for the L-31N and Snapper Creek Extension Canals indicates that the deviations between the 1-D and 2-D K are larger at the more narrow Snapper Creek Extension Canal cross sections. This correlates well with the predictions from theory and the hypothetical channel cases. The magnitude of deviations at the Snapper Creek Extension Canal sites are greater than the smallest errors in the UVM line-velocity measurements, indicating that 2-D effects may be significant at some UVM sites, especially those with narrower, deeper cross sections. A comparison of UVM discharges at L-31N Canal, calculated with the 1-D and 2-D K values and discharges determined with a Neil Brown point acoustic velocity meter, resulted in the 2-D K producing results closer to those of the Neil Brown meter than the 1-D K. However, significant differences in the UVM meter results and the Neil Brown meter results still exist.

The equation presented in this report is a useful tool in estimating the effects of the assumptions made in K coefficient calculations because it accounts for lateral velocity variations in channel downstream velocity, and it can accommodate a corrected expression for the ratio of average velocity to measured velocity. Also, the equation requires none of the discretization of vertical area slices in the channel cross section needed in its 1-D counterpart. Its disadvantage lies in its limited channel cross-section curve-fitting ability. It can be used to identify the trend of the errors in the 1-D equation and indicate the conditions under which the errors are most significant, but its use as a replacement for the 1-D equation is not warranted at this time due to the curve-fitting limitation. Additional work is needed to develop more sophisticated equations expressing the 2-D velocity profile in the K coefficient equation that will produce more accurate curve fits for the cross sections. Only then could the 2-D K coefficient replace the 1-D K.

REFERENCES CITED

Chin, D.A., 1990, A method to estimate canal leakage to the Biscayne aquifer, Dade County, Florida: U.S. Geological Survey Water-Resources Investigations Report 90-4135, 32 p.

Chiu, C.L., Hsiung, D.E., and Lin, H.C., 1978, Three dimensional open channel flow: Journal of the Hydraulics Division, American Society of Civil Engineers, v. 104, no. HY8, p. 1119-1136.

Chiu, C.L., Lin, H.C., and Mizumura, Kazumasa, 1976, Simulation of hydraulic processes in open channels: Journal of the Hydraulics Division, American Society of Civil Engineers, v. 102, no. HY2, p. 185-203.

Daugherty, R.L., Franzini, J.B., and Finnemore, E.J., 1985, Fluid mechanics with engineering applications: New York, McGraw Hill, 598 p.

Falvey, H.T., 1983, Effect of gradients on acoustic velocity meter: Journal of the Hydraulics Division, American Society of Civil Engineers, v. 109, no. 11, p. 1441-1460.

French, R.H., 1985, Open channel hydraulics: New York, McGraw-Hill, p. 34-37, 705 p.

Gupta, R.S., 1989, Hydrology and hydraulic systems: Englewood Cliffs, N.J., Prentice Hall.

Laenen, Antonius, 1985, Acoustic velocity meter system: U.S. Geological Survey Techniques of Water Resources Investigations, book 3, chap. A17, 38 p.

Laenen, Antonius, and Curtis, R.E., Jr., 1989, Accuracy of acoustic velocity metering systems for measurement of low velocity in open channels: U.S. Geological Survey Water-Resources Investigations Report 89-4090, 15 p.

Newman, J.D., 1982, Advances in gauging open channels and rivers using ultrasonic and electromagnetic methods: International Symposium on Hydrometeorology, American Water Resources Association.

Rantz, S.E., and others, 1982, Measurement and computation of streamflow: Volume 1—Measurement of stage and discharge: U.S. Geological Survey Water-Supply Paper 2175, 284 p.